

Article

Comprehensive Utilization of Pyrite Concentrate Pyrolysis Slag by Oxygen Pressure Leaching

Lin-Bo Liu , Longsheng Yi and Yunfeng Song *

School of Minerals Processing and Bioengineering, Central South University, Changsha 410083, China; csuliulinbo@163.com (L.-B.L.); cmiyls@163.com (L.Y.)

* Correspondence: syfeng@csu.edu.cn; Tel.: +86-0731-8883-0482

Abstract: The preparation of high-purity sulfur and pyrrhotite by pyrolysis holds great potential to realize the high-value utilization of pyrite concentrate (FeS_2), i.e., a by-product during the flotation of sulfide ore. In this study, the pyrrhotite obtained from the pyrolysis of pyrite concentrate was taken as the study object, and the effects of acid types, initial acidity, leaching time, leaching temperature, oxygen pressure, and liquid-to-solid ratio on the leaching behavior of pyrrhotite under oxygen pressure, were explored. The results show that elemental sulfur and hematite-based iron residue can be obtained by oxygen pressure leaching of pyrrhotite. It is found that the optimal experimental conditions for pyrrhotite oxygen pressure leaching are hydrochloric acid with 0.8 mol/L of initial acidity, 5 h of leaching time, 0.8 MPa of oxygen partial pressure, and 9:1 of liquid to solid ratio at 150 °C; moreover, the yield of sulfur reached 88.37%. Under optimal conditions, the leaching ratios of Fe, Pb, and Zn were 19.8%, 92.25%, and 99.11%, respectively. The sieved leaching residue was roasted at a low temperature of 500 °C, where the grade of Fe in the obtained hematite iron powder was 61.46%, and the grades of Pb, Zn, and S were 0.082%, 0.024%, and 0.1%. Clearly, the results meet well with the standard of the first grade of pyrite cinder, and this process realizes the comprehensive recovery of Fe and S resources in pyrolysis slag, which provides a superb technical route for the high-value utilization of pyrite concentrate.

Keywords: pyrolytic slag of pyrite concentrate; oxygen pressure leaching; elemental sulfur; hematite



Citation: Liu, L.-B.; Yi, L.; Song, Y. Comprehensive Utilization of Pyrite Concentrate Pyrolysis Slag by Oxygen Pressure Leaching. *Minerals* **2023**, *13*, 726. <https://doi.org/10.3390/min13060726>

Academic Editor: Benjamin P. Wilson

Received: 11 May 2023
Revised: 22 May 2023
Accepted: 24 May 2023
Published: 25 May 2023



Copyright: © 2023 by the authors. Licensee MDPI, Basel, Switzerland. This article is an open access article distributed under the terms and conditions of the Creative Commons Attribution (CC BY) license (<https://creativecommons.org/licenses/by/4.0/>).

1. Introduction

Pyrite concentrate (FeS_2) is an important by-product obtained from sulfide ore flotation, which is mainly used to produce sulfuric acid [1,2]. The pyrite concentrate obtained from lead–zinc flotation contains high levels of impurity elements (e.g., lead and zinc), which pose a serious problem for the traditional acid-making process. Moreover, the current surplus in the sulfuric acid market has limited the sales of sulfuric acid, resulting in a large accumulation of pyrite concentrates [3]. Due to its high impurity content, pyrite slag produces complex iron phases that are harmful to subsequent iron refining processes, rendering it effectively unusable [4–6]. Although different methods (e.g., magnetic separation, gravity separation [7], flotation [8], and magnetic roasting [9]) have been developed to recover iron from pyrite slag, they suffer from high energy consumption and production costs [10], and it is difficult to reduce impurity elements to the required level in the final product. This leads to poor comprehensive utilization of iron and sulfur resources, and significantly reduces the value of pyrite concentrate [11–13]. Moreover, the traditional roasting method for acid production normally generates flue gas and roasted slag from long-term storage, which could lead to serious environmental issues [14,15]. Therefore, developing a green and efficient way to realize the high-value utilization of pyrite concentrate has never been more imperative.

Currently, the sulfur market in China is in short supply [16], and thus recovering sulfur from pyrite concentrate in the form of elemental sulfur is expected to realize the high-value

utilization of pyrite concentrate. Nevertheless, effective methods to obtain elemental sulfur from concentrate have not yet been developed.

According to the Θ -pH diagram of metal sulfides, it is known that the properties of FeS₂ are quite stable and theoretically require a pH of less than -2 to achieve optimal leaching, while FeS is more reactive and would be leached at a pH greater than 1 [17–19]. Through screening the literature [20], metal sulfides (e.g., FeS₂ and MoS₂) with a metal-to-sulfur atomic ratio of 1:2 are classified as sulfate ion-forming sulfides, and oxygen pressure leaching only produces SO₄²⁻ from these sulfides, while metal sulfides (e.g., CuFeS₂, ZnS, PbS and Fe₇S₈) with a metal-to-sulfur atomic ratio close to or greater than 1:1 are classified as elemental sulfur-forming sulfides [21], and oxygen pressure leaching of these sulfides could produce elemental sulfur with a yield approaching 100% [22]. This suggests that if pyrite concentrate can be pyrolyzed to remove parts of sulfur, then sulfur products and pyrolytic slag pyrrhotite can be obtained, and the slag can be further processed through oxygen pressure acid leaching to obtain sulfur, and the concurrently obtained hematite can be further processed into iron concentrate [23]. Thus, the thermal decomposition–oxygen pressure leaching process can potentially achieve the high-value utilization of iron and sulfur resources in pyrite concentrate.

In our previous experiments, we obtained high-purity sulfur (99.5%) and pyrrhotite pyrolysis slag by pyrolyzing pyrite concentrate at high temperatures (600–700 °C) under an inert atmosphere of N₂ [24]. The main objective of this study is to investigate the behavior of magnetic pyrrhotite in oxygen pressure leaching of pyrolysis slag. More specifically, the effects of hydrochloric and sulfuric acid on oxygen pressure leaching products were initially compared, suitable acid reagents were chosen, and the effects of initial acidity, leaching time, leaching temperature, oxygen partial pressure, and liquid-to-solid ratio on the sulfur yield, iron residue morphology, and partitioning behaviors of valuable elements in the two phases were subsequently investigated using single-factor conditional experiments. Simultaneously, X-ray diffraction (XRD) was conducted to elucidate the phase transformation mechanism under different oxygen pressure leaching conditions of magnetic pyrite. Consequently, the residue phase was subjected to a purification process and a process flowchart for the utilization of pyrite concentrate was proposed. This paper beyond any doubt offers a potential green and economic technological route for the high-value utilization of pyrite concentrate.

2. Materials and Methods

2.1. Materials

The pyrite concentrate originated from a lead–zinc mine in Hunan, China, and the slag was obtained by pyrolyzing pyrite concentrate at high temperatures (600–700 °C) under an inert atmosphere of (N₂). The composition of the blended pyrolysis slag sample is presented in Table 1.

Table 1. The chemical multi-element analysis of the pyrolysis slag.

| Element | Fe | S | Pb | Zn | Mg | Si | Ca | As | Al | C | K | Others |
|----------------|-------|-------|------|------|-------|------|------|--------|------|-------|------|--------|
| Content (wt.%) | 54.26 | 36.70 | 0.78 | 0.36 | 0.095 | 2.16 | 1.35 | 0.0073 | 0.38 | 0.037 | 0.16 | 3.7107 |

Clearly, Table 1 reveals that the pyrolysis slag is primarily composed of Fe, S, Pb, and Zn, where Fe accounts for 54.26% of the total composition, followed by S at 36.70%, Pb at 0.78%, and Zn at 0.36%. The XRD pattern of the pyrolysis slag in Figure 1 indicates that the main iron-bearing phase is pyrrhotite.

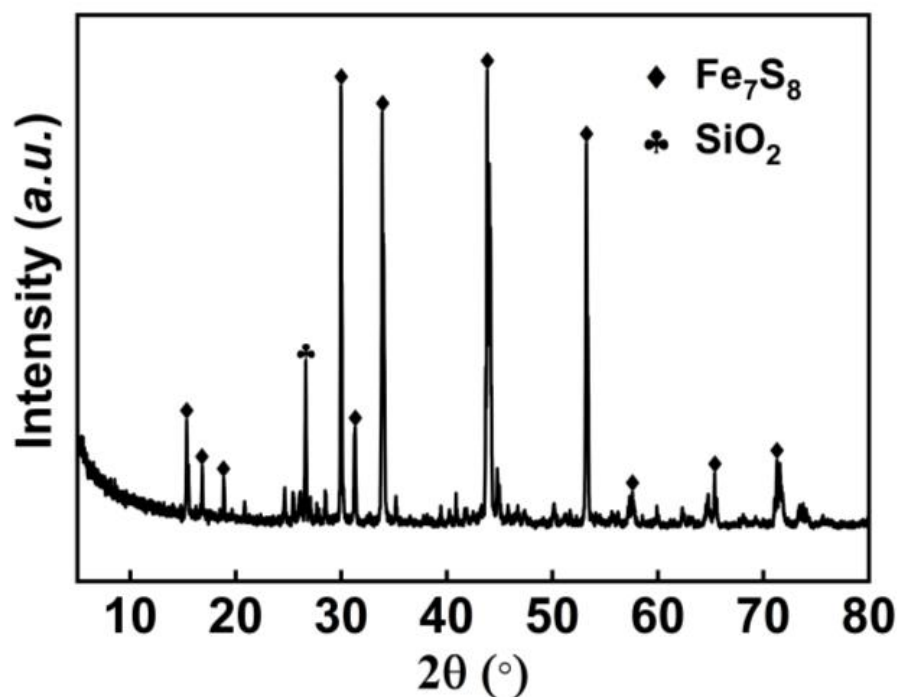


Figure 1. XRD patterns of the pyrolysis slag.

2.2. Experimental Procedures

The pyrolysis slag was ball milled and sieved to ensure that more than 95% of the particles had a size below 50 μm . A solid-to-liquid ratio of the pyrolysis slag (30 g with a theoretical sulfur content of 11 g) with hydrochloric (or sulfuric) acid and water, was added to the autoclave (LC-KH-200, 200 mL with stainless steel housing and Teflon lining, LiChen Instrument Technology Co., Shanghai, China), which was subsequently sealed to ensure gas tightness. The mixture was then stirred and heated with oxygen passing through. Upon completion of the oxygen pressure leaching process, the slurry inside the autoclave was pumped out and subjected to vacuum filtration to separate the liquid and solid components. The leachate was kept sealed and the leaching residue was placed in a vacuum drying oven at a certain temperature of 70 $^{\circ}\text{C}$ for 12 h for further characterization. The detailed process parameters of the study on the utilization of the pyrrhotite pyrolysis slag under various leaching conditions are shown in Table 2. Moreover, the obtained leaching residue was roasted under air at 500 $^{\circ}\text{C}$ for 2 h with heating rates of 10 $^{\circ}\text{C}/\text{min}$ to obtain pyrite cinder first grade.

Table 2. Process parameters to study the effects of different leaching conditions.

| Effects/Leaching Conditions | Acid Types | Initial Acidity/mol/L | Leaching Temperature/ $^{\circ}\text{C}$ | Leaching Time/h | Oxygen Pressure/Mpa | Liquid-to-Solid Ratio |
|-----------------------------|--------------------------------|-----------------------|--|-----------------|---------------------|-----------------------|
| Different acid types | Sulfuric/ hydrochloric acid | 0.8 | 140 | 4 | 1 | 15:1 |
| Initial acidity | Hydrochloric acid | 0.5/0.6/0.8/1.2/1.5 | 140 | 4 | 1 | 15:1 |
| Leaching time | Hydrochloric acid | 0.8 | 140 | 2/3/3.5/4/5 | 1 | 15:1 |
| Leaching temperature | Hydrochloric acid | 0.8 | 120/130/140/150/160 | 5 | 1 | 15:1 |
| Oxygen pressure | Hydrochloric acid | 0.8 | 150 | 5 | 0.4/0.6/0.8/1.0 | 15:1 |
| Liquid-to-solid ratio | Hydrochloric acid | 0.8 | 150 | 5 | 0.8 | 3:1/6:1/9:1/12:1/15:1 |

2.3. Characterization Methods

XRD (X'Pert3 Powder, PANalytical, Alemelo, The Netherlands) with Cu K α radiation (40 kV, 44 mA) was used to characterize the phase of the leaching residues. An inductively coupled plasma optical emission spectrometer (ICP, Spectro Blue, SPECTRRO Analytical, Kleve, Germany) was used to analyze the element (Fe, Zn, and Pb) content in the leaching solution. The frequency and power of the isotropic generator are 27.12 MHz and 700–1700 W, respectively. Carbon and sulfur concentrations are measured by a carbon and sulfur analyzer and other element concentrations were determined by atomic absorption spectrometry (AA6800, Shimadzu, Kyoto, Japan).

3. Results and Discussion

3.1. Leaching Conditions

3.1.1. Effect of Different Acid Types

Sulfuric acid and hydrochloric acid are commonly utilized for leaching. Herein, the effects of hydrochloric and sulfuric acid on the pressure leaching were investigated and the related results are shown in Table 3 and Figure 2.

Table 3. The pressure leaching products with different acid types.

| Acid Types | Red Pressure Leaching Residue/g | Fe in Leaching Residue/wt. % | Bulk Sulfur/wt. % | Powdered Sulfur/wt. % | Fe in Leaching Solution/wt. % |
|-------------------|---------------------------------|------------------------------|-------------------|-----------------------|-------------------------------|
| Hydrochloric acid | 23.21 | 66.57 | 23.64 | 54.27 | 33.43 |
| Sulfuric acid | 21.96 | 58.92 | 35.09 | 39.45 | 41.08 |

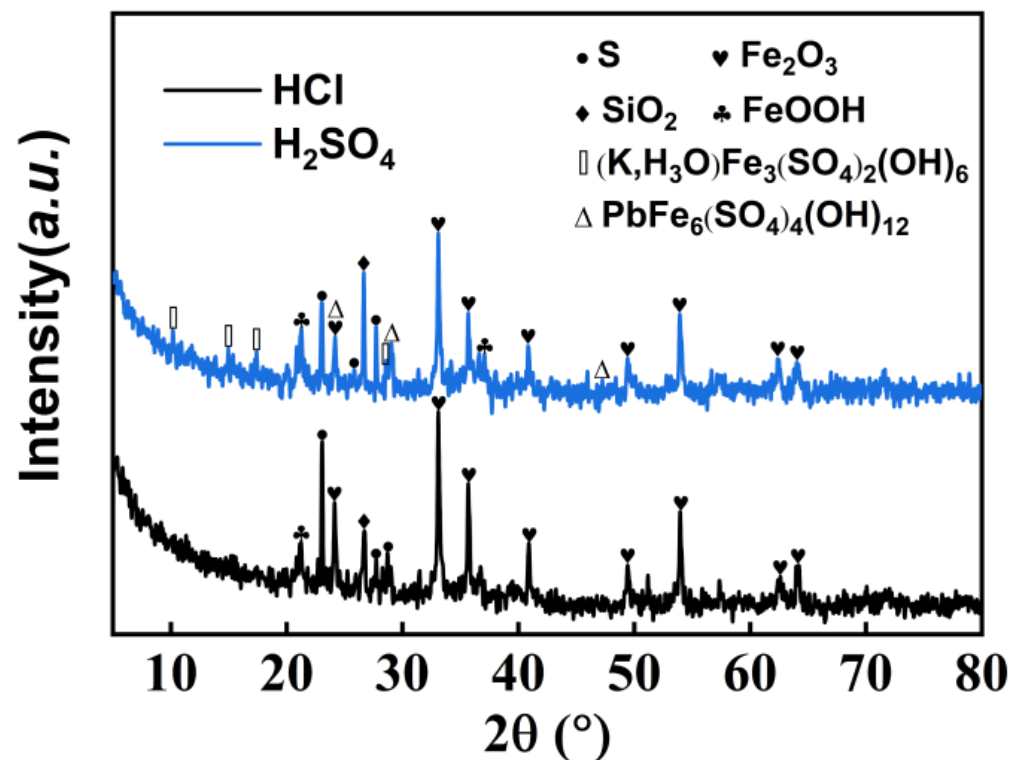


Figure 2. XRD patterns of the hydrochloric acid and sulfuric acid on red pressure leaching residue.

Based on the results shown in Table 3, it is evident that the leaching ratio of iron is marginally lower and the sulfur yield is slightly higher when the hydrochloric acid is used, as compared to the sulfuric acid. Furthermore, Figure 2 reveals that the use of sulfuric acid results in a more complex iron phase in the red pressure leaching residue, where numerous stray peaks appear, which could be attributed to the high sulfate content. This indicates that a portion of iron in the form of $(K, H_3O)Fe_3(SO_4)_2(OH)_6$ and $PbFe_6(SO_4)_4(OH)_{12}$ exists, which makes the subsequent iron recovery more challenging. In light of these findings, it can be concluded that hydrochloric acid proved to be a more suitable reagent for the oxygen pressure leaching of pyrrhotite. Therefore, hydrochloric acid was selected for leaching for further experiments.

3.1.2. Effect of Initial Acidity

The initial acidity of the used acid has a significant effect on the leaching rate and leaching ratio. Therefore, the effect of initial acidity on oxygen pressure leaching of pyrrhotite was investigated to obtain an optimal initial acidity, and the test results are shown in Figures 3–5.

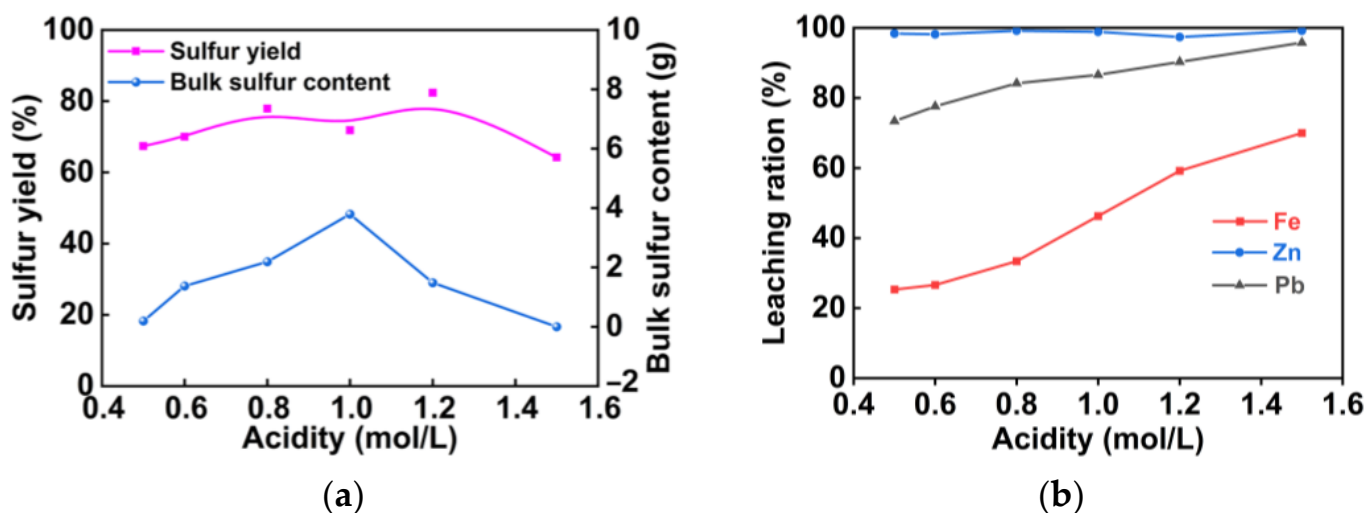


Figure 3. The effect of the initial acidity on oxygen pressure leaching of pyrrhotite: (a) sulfur yield and bulk sulfur content; (b) leaching ratios of Fe, Pb, and Zn.



Figure 4. Images of the pressure leaching products with different initial acidity.

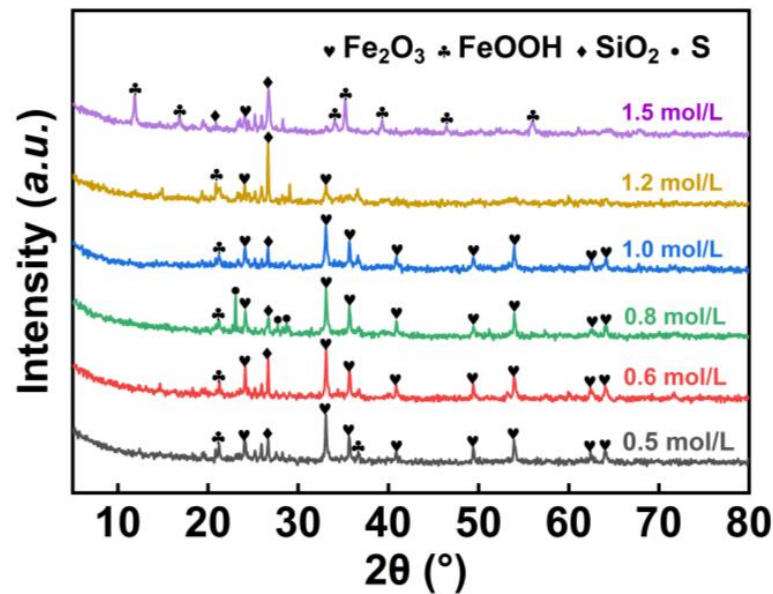


Figure 5. XRD patterns of the red pressure leaching residue with different initial acidity.

The leaching residues at different acidities are shown in Figure 4. The bulk sulfur yield is only 0.2 g at a 0.5 mol/L acidity. With the increase in initial acidity, the yield of bulk sulfur significantly increased, which could be attributed to the initial acidity of acid changing the surface tension of the sulfur, making it agglomerate.

As shown in XRD patterns (Figure 5), pyrrhotite peaks are absent at a 0.5 mol/L acidity, indicating successful leaching of pyrrhotite at a low pH. Upon increasing the acidity, peaks of hematite become more prominent. As the acidity increases beyond 1 mol/L, hematite peaks diminish and goethite peaks rise. Thus, an initial acidity of 0.8 mol/L was selected to minimize the iron leaching and to optimize the sulfur yield. The results show that, under this acidity, the sulfur yield was 78.4% with 2.6 g of bulk sulfur, and iron leaching was 33.4%, while the lead and zinc leaching were 84.1% and 99.0%, respectively.

3.1.3. Effect of Leaching Time

In hydrometallurgy production, the residence time of minerals in the high-pressure reactor is an important factor that affects the leaching ratio. This study investigates the effect of leaching time on the oxygen pressure leaching of pyrrhotite based on an acidity experiment and the results are presented in Figures 6–8.

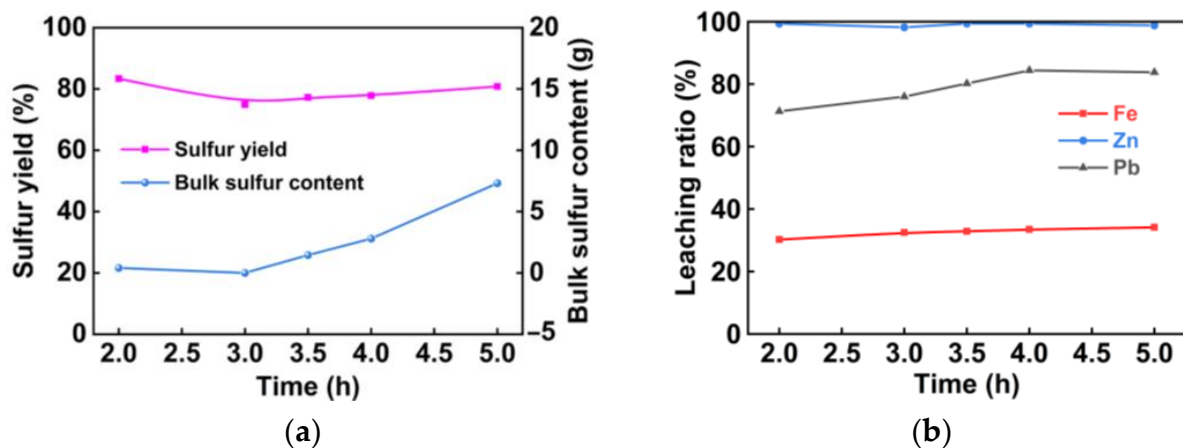


Figure 6. The effect of the leaching time on oxygen pressure leaching of pyrrhotite: (a) sulfur yield and bulk sulfur content; (b) leaching ratios of Fe, Pb, and Zn.



Figure 7. Images of the pressure leaching products with different leaching times.

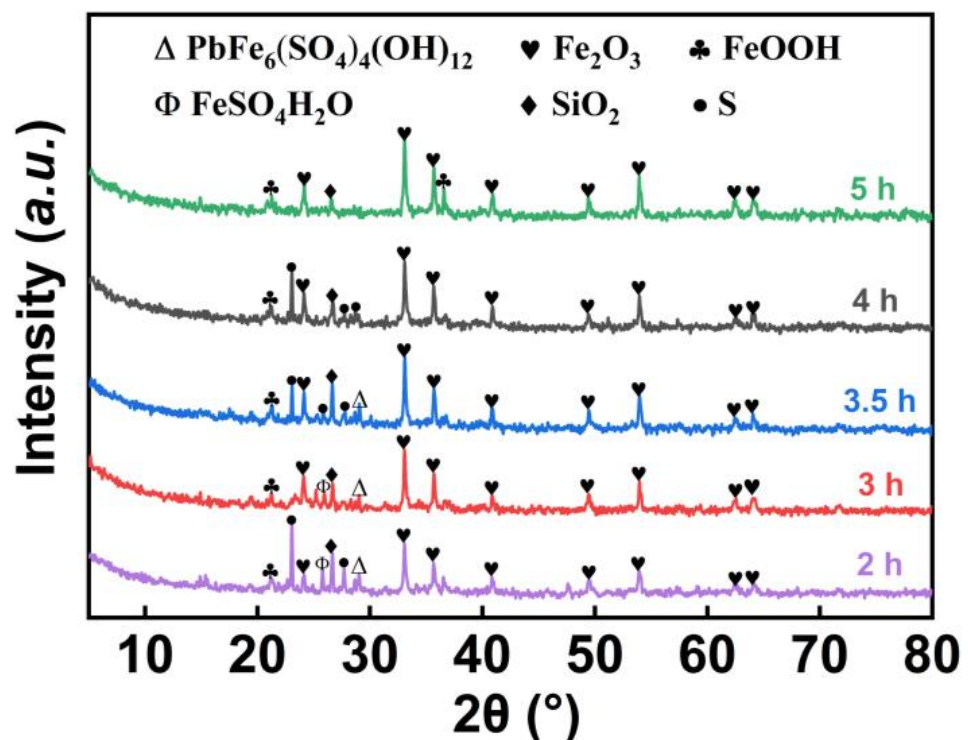


Figure 8. XRD patterns of the red pressure leaching residue with different leaching times.

Figures 6a and 7 displayed that the leaching time has a significant effect on the formation of the bulk sulfur. Clearly, no bulk sulfur was formed when the leaching time was 2 h, indicating that the leached elemental sulfur has not yet condensed into a solid block. As the leaching time increased, the liquid sulfur gradually accumulated into a solid block, leading to an increase in the content of bulk sulfur. With a leaching time of 5 h, the bulk sulfur content exceeded 7.86 g, and the sulfur yield reached 80.84%, where the sulfur quality obtained under these conditions was the best. According to Figure 6b, the leaching ratio of iron remains at approximately 33% as the leaching time increased from 2 to 5 h, and that of the lead remained between 70% and 85%, while that of the zinc remained at around 99%. It can be observed from the XRD pattern in Figure 8 that when the leaching time was short, iron may exist partially in the form of jarosite [i.e., $\text{KFe}_3(\text{SO}_4)_2(\text{OH})_6$], with other impurities. Especially at 5 h, the peaks of Fe_2O_3 in the XRD pattern are mostly consistent with the standard pattern, and the impurity peaks were less pronounced. Therefore, a leaching time of 5 h was considered to be the optimal condition.

3.1.4. Effect of Leaching Temperature

During the pressurized oxidation process, the temperature is a crucial factor that significantly affects the acid leaching results. The products obtained from oxygen pressure leaching of pyrrhotite mainly depend on the used temperature. When the temperature was between 180–200 °C and the oxygen partial pressure was 1.5–3.0 MPa, the sulfur present in pyrrhotite would be converted into SO_4^{2-} . Conversely, at a lower temperature of 100–150 °C, pyrrhotite could be oxidized to produce elemental sulfur [25]. This section mainly investigated how temperature affected the oxygen pressure leaching of pyrrhotite. The results are shown in Figures 9–11.

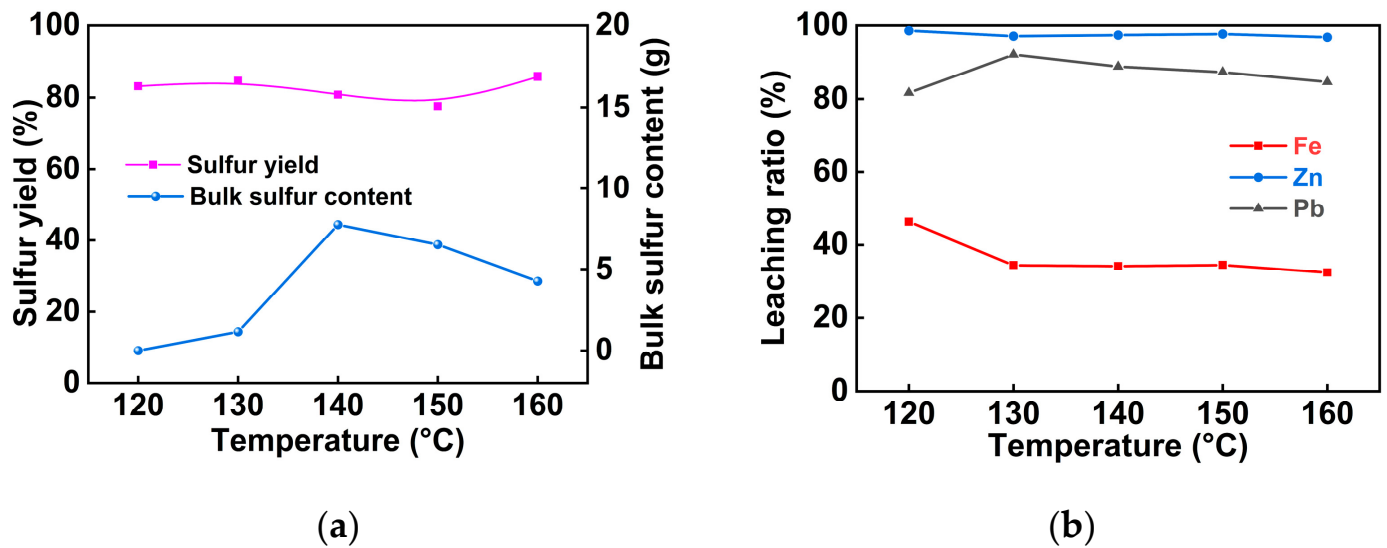


Figure 9. The effect of the leaching temperature on oxygen pressure leaching of pyrrhotite: (a) sulfur yield and bulk sulfur content; (b) leaching ratios of Fe, Pb, and Zn.

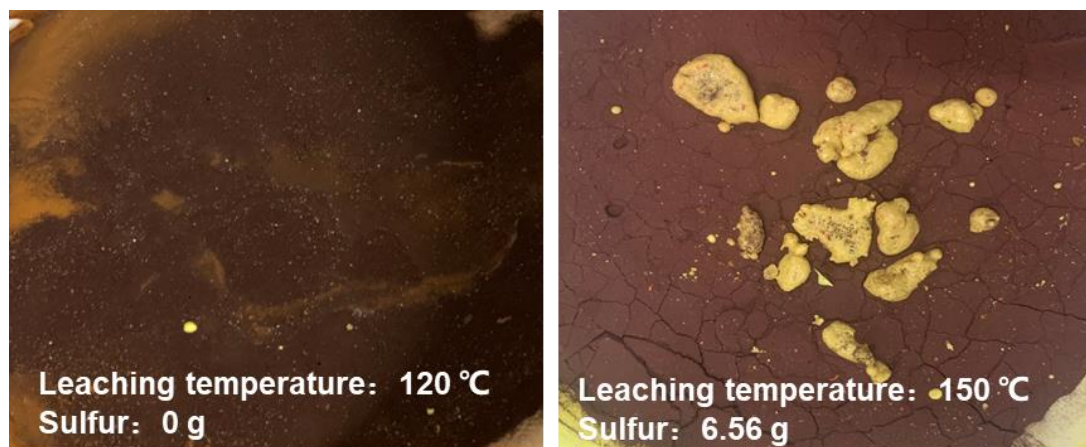


Figure 10. Images of the pressure leaching products at different leaching temperatures.

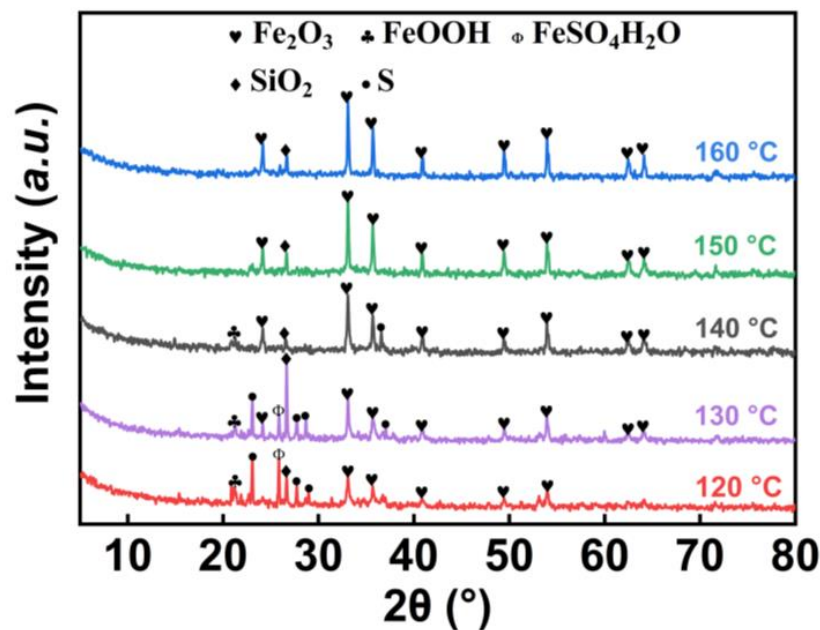


Figure 11. XRD patterns of the red pressure leaching residue at different leaching temperatures.

As shown in Figure 9a, the yield of elemental sulfur remained relatively stable at the temperature range of 120–160 °C, which maintained a value of over 78%. However, the yield of bulk sulfur exhibited significant fluctuations, i.e., an initial increase followed by a decrease as the temperature increases. Figure 10 illustrates that almost no bulk sulfur was produced at 120 °C, and all sulfur remained in a dispersed powder form within the leach residue. In contrast, 6.56 g of bulk sulfur was produced at 150 °C. Moreover, the viscosity of the liquid sulfur increases dramatically when the temperature reached 160 °C, making it challenging to be collected in the kettle. As a result, the yield of bulk sulfur significantly decreased. As shown in Figure 9b, incomplete leaching of pyrrhotite occurred at 120 °C due to the lower temperature, resulting in the presence of divalent Fe in the solution with a relatively higher Fe leaching ratio of 46.28%. As the temperature increased, Fe ions underwent further oxidation to form hematite, and only about 34% of the Fe was leached at 160 °C, resulting in the least amount of Fe loss. The leaching ratio of Pb remained in the range of 80% to 90% at the temperature range of 120–160 °C.

Figure 11 displays the XRD patterns of the red pressure leaching residue obtained at various temperatures. Through a close inspection of all the XRD results, it is found that the intensity of the hematite peak and the crystalline purity increased as the temperature increased. Additionally, the area of the hematite peaks gradually enlarged, while the spurious peaks of other iron phase compounds diminished. After a comprehensive evaluation, a leaching temperature at 150 °C was demonstrated to be an optimal value, where the sulfur yield was 78.1%, the bulk sulfur yield was 6.56 g, the leaching ratio of Fe was only 34.4% and the iron loss was minimized.

3.1.5. Effect of Oxygen Pressure

Oxygen pressure is another key parameter in the production of hematite through pyrrhotite leaching, and the effect of oxygen partial pressure on oxygen pressure leaching of pyrrhotite was studied by controlling the optimal initial acidity, leaching time, and temperature obtained from previous experiments. The specific experimental results are shown in Figures 12–14.

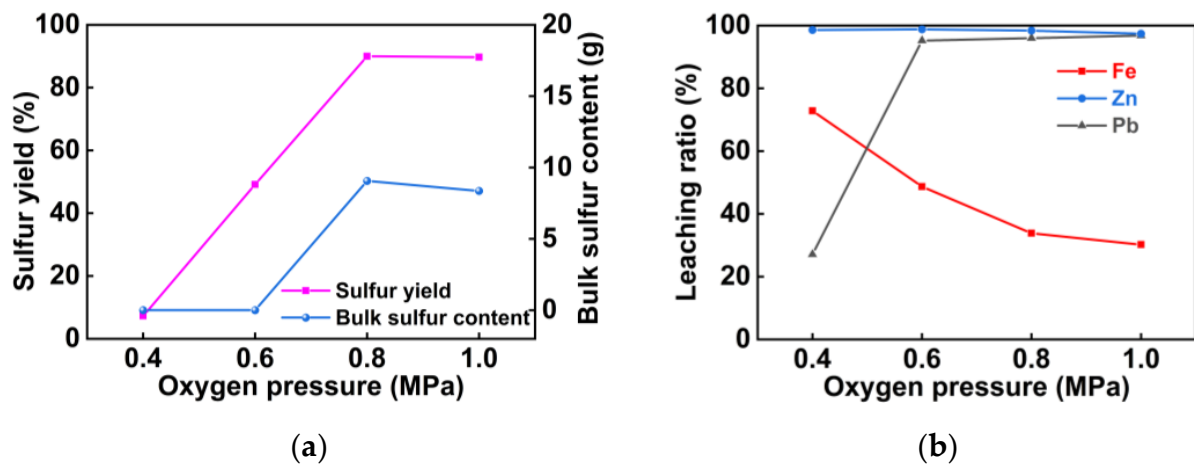


Figure 12. The effect of oxygen pressure on oxygen pressure leaching of pyrrhotite: (a) sulfur yield and bulk sulfur content; (b) leaching ratios of Fe, Pb, and Zn.



Figure 13. Images of the pressure leaching products at different oxygen pressure.

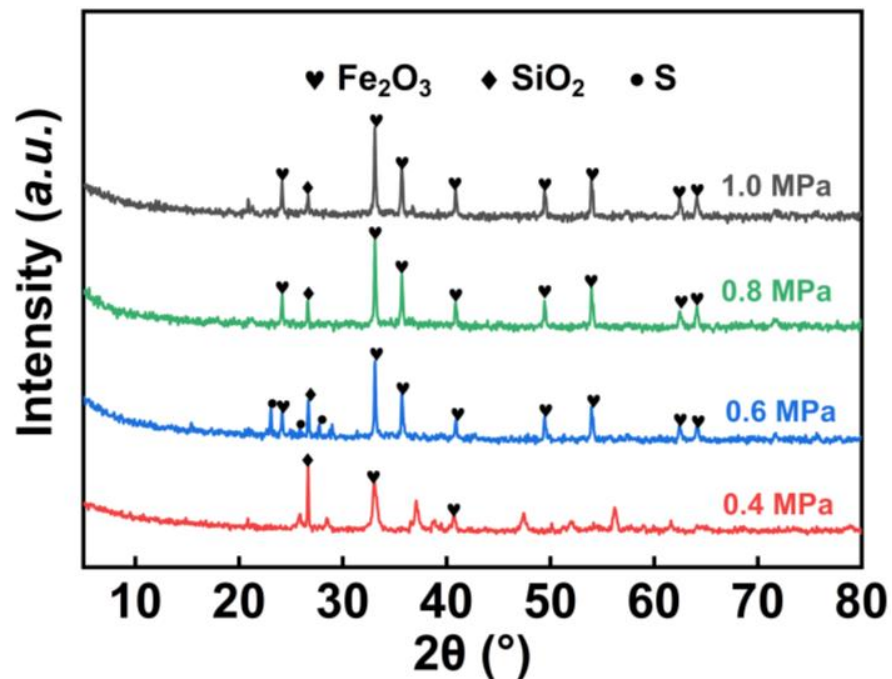
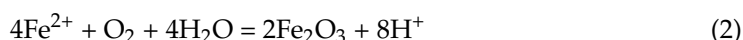
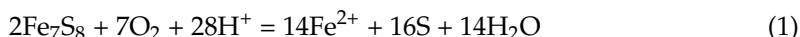


Figure 14. XRD patterns of the red pressure leaching residue with different oxygen pressure.

It can be seen in Figures 12a and 13 that when the oxygen pressure is 0.4 MPa, it is not enough to leach sulfur, which enables a quite low sulfur yield, and the residue was black, indicating that almost no hematite was generated. With the continuous increase in

oxygen pressure, the sulfur yield and bulk sulfur gradually increased. At 0.8 MPa, the sulfur quality was the best, which was quite easy to be separated from the red residue. Figure 12b shows that the leaching ratio of iron gradually decreases with oxygen pressure, and iron was gradually oxidized into hematite. When the oxygen pressure was 0.4 MPa, the leaching ratio of iron reached 72.83%, which indicated that the acid is basically used to decompose pyrrhotite, while the PbS was difficult to be leached with a value of only 27.71%. Furthermore, the oxidation of iron ions continued with the increase in oxygen pressure. According to Equations (1) and (2), the oxidation process of iron would produce acid, which increased the leaching ratio of lead.



According to the XRD patterns of leaching residue (Figure 14), the pyrrhotite was gradually leached and the hematite peak was gradually sharpened with the increase in oxygen partial pressure. When the oxygen partial pressure was 0.8 MPa, as compared to other conditions, the leaching residue showed fewer miscellaneous peaks, and the hematite possessed the highest crystalline purity. This suggested that 0.8 MPa was the optimal oxygen pressure condition with a comprehensive consideration, where the highest sulfur yield was 90%, together with a bulk sulfur yield of 8.96 g and a Fe leaching ratio of only 33.82%.

3.1.6. Effect of Liquid-to-Solid Ratio

The liquid-to-solid ratio, as another important economic and technical parameter in the hydrometallurgical leaching process, was further investigated. It is well known that a high liquid-to-solid ratio could reduce the viscosity of the slurry at a certain concentration of leaching agent, which is beneficial for improving the leaching ratio. However, an excessive liquid-to-solid ratio could result in a high requirement for liquid-solid separation equipment, which inevitably results in an undesirable economic burden. Therefore, an optimal liquid-to-solid ratio often needs to be determined through experimental investigation. On the basis of the abovementioned studies, the effect of the liquid-to-solid ratio on the oxygen pressure leaching of pyrrhotite was thus explored. The experimental results are shown in Figures 15–17.

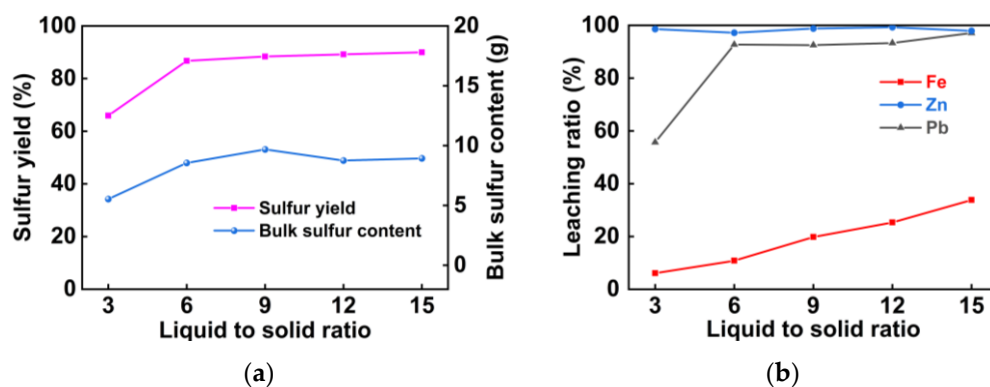


Figure 15. The effect of liquid-to-solid ratio on oxygen pressure leaching of pyrrhotite: (a) the sulfur yield and bulk sulfur content; (b) the leaching ratios of Fe, Pb, and Zn.



Figure 16. Images of the pressure leaching products with different liquid-to-solid ratios.

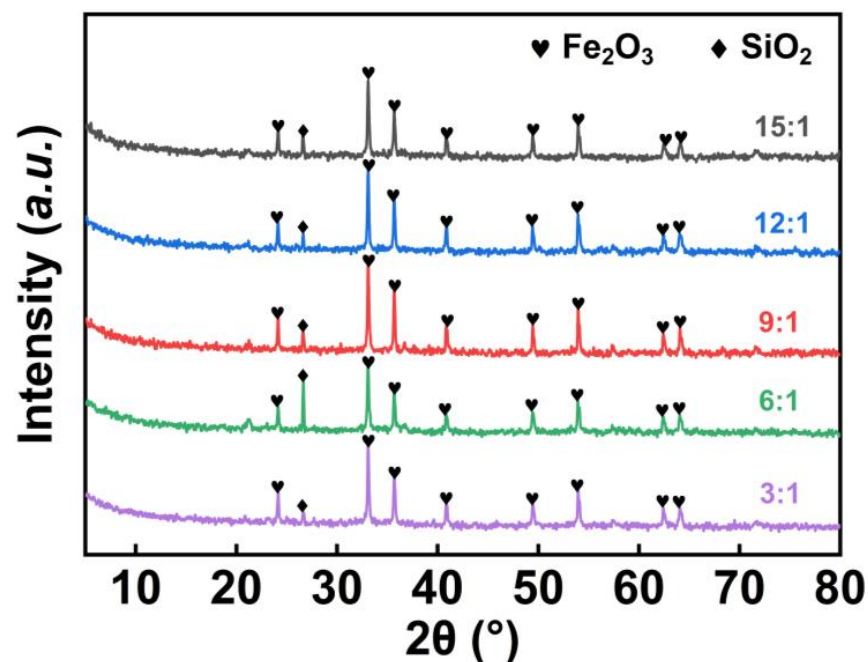


Figure 17. XRD patterns of the red pressure leaching residue with different liquid-to-solid ratios.

It can be seen that the viscosity of the slurry was too high when the liquid-to-solid ratio was 3:1 (Figure 15a), which was not conducive to the mass transfer since an agglomeration phenomenon was observed (Figure 16), where the sulfur yield and the bulk sulfur content were both low. Clearly, a decrease in the viscosity of the slurry could improve the sulfur yield and bulk sulfur content as the liquid-to-solid ratio increased. Moreover, the liquid-to-solid ratio of 9:1 only achieved bulk sulfur, and negligible changes were observed in the sulfur yield and the bulk sulfur production when the liquid-to-solid ratio was further increased. In the meantime, the acid content gradually increased as the liquid-to-solid ratio increased (Figure 15b), and the leaching ratios of iron and lead continued to rise. However, an excessive liquid-to-solid ratio was not conducive to the recovery of iron elements.

It can be observed from the XRD patterns in Figure 17 that the hematite peaks in the red residue were the strongest ones and the miscellaneous peaks were the lowest, suggesting that the content of hematite in the red residue was quite high, which was close to a value of over 90%. It is thus believed that the optimal liquid-to-solid ratio was 9:1.

In light of all the studies involving acid type, initial acidity, leaching time, leaching temperature, oxygen pressure, and liquid-to-solid ratio, it is determined that the optimal test conditions for pressurized oxidation acid leaching of pyrolysis slag are determined to be an initial acidity of 0.8 mol/L of hydrochloric acid, a leaching time of 5 h, an oxygen partial pressure of 0.8 MPa and a liquid to solid ratio of 9:1 at a temperature of 150 °C.

With all the optimal leaching conditions, the sulfur yield achieved a value of 88.37%, and all sulfur was bulk sulfur with a value of 9.71 g. Moreover, the leaching ratio of iron in the slag was only 19.8%, while the leaching ratios of Pb and Zn were 92.25% and 99.11%, respectively.

3.2. Preparation of Target Products

The crude sulfur product and hematite leaching residue were obtained from the pyrolysis slag through oxygen pressure leaching. The content of elemental sulfur in the crude sulfur product obtained under the optimal conditions was 96.6%, and its grade could be further improved to meet the standard of first-class products by means of hot melting and other methods. In addition, the elemental content of the red leaching residue after a simple screening was tested, and the results are shown in Table 4.

Table 4. Quantitative analysis of elements of pressure leaching residue.

| Element | S | Fe | Pb | Zn | Others |
|-------------|------|-------|-------|-------|--------|
| Content (%) | 0.22 | 55.14 | 0.079 | 0.019 | 44.542 |

It can be seen that the leaching residue contained 0.22% of elemental sulfur, and the iron grade was 55.14%, as illustrated in Table 4. Therefore, the obtained leaching residue of hematite was roasted at a low temperature of 500 °C, and the XRD patterns of the roasted slag were shown in Figure 18, where only characteristic peaks of hematite and silica appeared in the slag, indicating that small amounts of goethite and alum were transformed into hematite. Concurrently, the sulfur content of the leaching residue was reduced, and the quality of hematite was greatly improved.

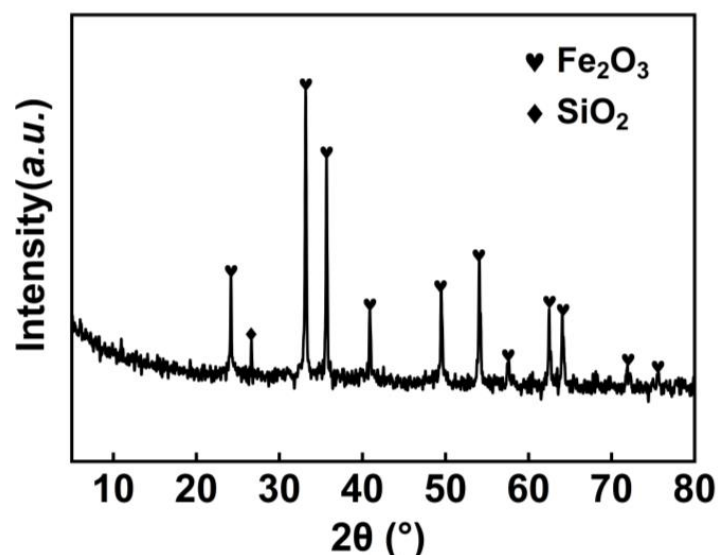


Figure 18. XRD pattern of the roasted leaching residue.

The element analyses of the roasted leaching residue are shown in Table 5. It shows that the Fe grade was 61.46%, the S grade was 0.1%, and the content of Pb and Zn was 0.106%, all of which were well in line with the first-grade iron concentrate for the GB/T 29502-2013 of pyrite cinder (Table 6).

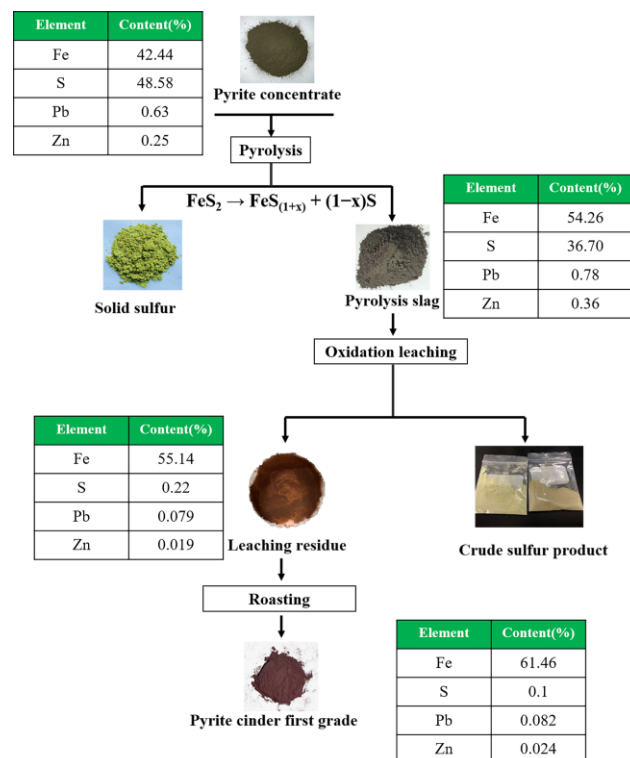
Table 5. Quantitative analysis of elements in hematite.

| Element | S | Fe | Pb | Zn | Others |
|-------------|-----|-------|-------|-------|--------|
| Content (%) | 0.1 | 61.46 | 0.082 | 0.024 | 38.334 |

Table 6. Chemical composition of pyrite cinder (GB/T 29502-2013).

| Grade | Chemical Composition (%) | | | | | | |
|--------------|--------------------------|------------------|------|-------|-------|------|---------|
| | TFe | SiO ₂ | S | P | As | Cu | Pb + Zn |
| First-grade | ≥60.0 | ≤6.0 | ≤1.0 | ≤0.05 | ≤0.05 | ≤0.2 | ≤0.3 |
| Second-grade | ≥58.0 | ≤10.0 | ≤1.5 | ≤0.08 | ≤0.08 | ≤0.3 | ≤0.5 |
| Third-grade | ≥54.0 | ≤12.0 | ≤2.5 | ≤0.12 | ≥0.12 | ≤0.4 | ≤1.0 |

To sum up, the process of pyrolysis-oxygen pressure leaching for comprehensive utilization of valuable elements of pyrite concentrate is shown in Figure 19. The Fe in the pyrite concentrate mainly exists in the form of FeS₂, with small amounts of FeCO₃, Fe₂O₃, and FeSiO₄, and Pb mainly exists in the form of PbSO₄ and PbS. By pyrolyzing the pyrite concentrates under the inert atmosphere, high-purity elemental sulfur and pyrolysis slag were obtained, where the pyrolysis slag could be further processed through oxygen pressure acid leaching to prepare sulfur crude products and leaching residue. The sulfur crude products could be further treated by hot melting (114 °C) to become liquid sulfur and separated from solid impurities to obtain high-grade sulfur. Moreover, after the leaching residue was roasted, qualified first-grade pyrite cinder could be obtained.

**Figure 19.** The process of pyrolysis-oxygen pressure leaching for comprehensive utilization of valuable elements in pyrite concentrate.

4. Conclusions

- (1) The phase of leaching residue obtained with hydrochloric acid is simpler and closer to hematite, while the iron phase of the autoclaved residue obtained with sulfuric acid is complex. In addition to hematite, there are goethite, alum, and other substances, which are more stringent for the subsequent roasting conditions;
- (2) Sulfur can be obtained through oxygen pressure leaching of pyrolysis slag. The yield of elemental sulfur significantly increases with oxygen pressure, and the bulk sulfur increases first and then decreases with initial acidity and temperature, and steadily increases with reaction time and oxygen pressure. The leaching ratio of iron increases

- with initial acidity and the liquid-to-solid ratio, and gradually decreases with oxygen pressure. The oxygen pressure leaching has a good effect on the leaching of Pb and Zn in the pyrolysis slag, where the leaching ratio reaches a value of more than 90%, while the content of Pb and Zn in hematite products is extremely low;
- (3) The optimal experimental conditions for oxygen pressure leaching of pyrolysis slag are determined to be an initial acidity of 0.8 mol/L, a leaching time of 5 h, an oxygen partial pressure of 0.8 MPa, a liquid-to-solid ratio of 9:1 at a temperature of 150 °C. Under these conditions, the yield of sulfur elemental reaches 88.37%, and the leaching ratio of Fe is only 19.8%, while the leaching ratios of Pb and Zn are 92.25% and 99.11%;
 - (4) After roasting the leached residue, the sulfur content in the hematite is reduced to 0.1%, and the content of Pb and Zn in the slag is 0.106%. The element content analysis result of the roasted slag well meets the standard of the first-grade pyrite cinder. Apparently, the proposed technical route holds great potential for the high-value utilization of pyrite concentrate.

Author Contributions: Conceptualization, L.-B.L.; Data curation, L.-B.L.; Funding acquisition, Y.S.; Investigation, L.-B.L.; Methodology, L.-B.L.; Project administration, Y.S.; Resources, Y.S.; Supervision, L.Y. and Y.S.; Writing—original draft, L.-B.L.; Writing—review & editing, Y.S. All authors have read and agreed to the published version of the manuscript.

Funding: This research was supported by the National Key R&D Program of China (2022YFC3900801, 2022YFC3900804), the National Natural Science Foundation of China (Grant Nos. 91962223 and 52104357), the Natural Science Foundation of Hunan province (2022JJ40612), the Young Elite Scientists Sponsorship Program by CAST (2022QNRC001), and the 2022 Chenzhou National Sustainable Development Demonstration Zone Project (2022sfq34).

Data Availability Statement: Data are available from the authors on request.

Acknowledgments: Many thanks to Subiao Liu for his helpful guidance.

Conflicts of Interest: The authors declare no conflict of interest.

References

1. Li, Y.L.; Guan, W.S.; Shi, X.D.; Wangm, Q.; Li, S.Q. Research advances in the reclamation of gold and silver from pyrite slag. *Appl. Chem. Ind.* **2009**, *11*, 1671–1674.
2. Oliveira, M.L.S.; Ward, C.R.; Izquierdo, M.; Sampaio, C.H.; Brum, I.A.S.; Kautzmann, R.M.; Sabedot, S.; Querol, X.; Silva, L.F.O. Chemical composition and minerals in pyrite ash of an abandoned sulphuric acid production plant. *Sci. Total Environ.* **2012**, *430*, 34–47. [[CrossRef](#)] [[PubMed](#)]
3. Zhang, Y.; Xing, D.; Wang, G.; Zeng, X.; Deng, Z. Technology and industrialization of sulphur recovery from pyrite and polymetallic sulfide ore. *Sulfuric Acid Ind.* **2018**, *1*, 13–16.
4. Alp, I.; Deveci, H.; Yazıcı, E.Y.; Türk, T.; Süngün, Y.H. Potential use of pyrite cinders as raw material in cement production: Results of industrial scale trial operations. *J. Hazard.* **2009**, *166*, 144–149. [[CrossRef](#)]
5. Zhang, J.F.; Yan, Y.; Hu, Z.H.; Fan, X.Z.; Zheng, Y. Utilization of low-grade pyrite cinder for synthesis of microwave heating ceramics and their microwave deicing performance in dense-graded asphalt mixtures. *J. Clean. Prod.* **2018**, *170*, 486–495. [[CrossRef](#)]
6. Tiberg, C.; Bendz, D.; Theorin, G.; Kleja, D.B. Evaluating solubility of Zn, Pb, Cu and Cd in pyrite cinder using leaching tests and geochemical modelling. *Appl. Geochem.* **2017**, *85*, 106–117. [[CrossRef](#)]
7. Abdrakhimova, E.S.; Abdrakhimov, V.Z. Study of combustion processes in firing of a heat-insulator produced from technogenic raw materials from nonferrous metallurgy and power industry. *Russ. J. Appl. Chem.* **2012**, *63*, 130–132. [[CrossRef](#)]
8. Liu, A.P.; Ni, W.; Wu, W. Mechanism of separating pyrite and dolomite by flotation. *J. Beijing Univ. Sci. Technol. Miner. Metall. Mater.* **2007**, *14*, 291–296. [[CrossRef](#)]
9. Chen, D.; Gou, H.; Lv, Y.; Li, P.; Yan, B.; Xu, J. Preparation and recovery of iron carbide from pyrite cinder by carburizing magnetic separation technology. *J. Min. Metall. Sect. B Metall.* **2018**, *54*, 271. [[CrossRef](#)]
10. Guo, Z.Q.; Pan, J.; Zhu, D.Q.; Yang, C.C. Mechanism of composite additive in promoting reduction of copper slag to produce direct reduction iron for weathering resistant steel. *Powder Technol.* **2018**, *329*, 55–64. [[CrossRef](#)]
11. Toubri, Y.; Plane, B.; Demers, I.; Fillion, M. Probing cleaner production opportunities of the Lac Tio pyrite-enriched tailings generated to alleviate sulfur dioxide emissions. *J. Clean. Prod.* **2022**, *357*, 132027. [[CrossRef](#)]
12. Jiang, T.; Tu, Y.; Su, Z.; Lu, M.M.; Liu, S.; Liu, J.C.; Gu, F.Q.; Zhang, Y.B. A new value-added utilization process for pyrite cinder: Selective recovery of Cu/Co and synthesis of iron phosphate. *Hydrometallurgy* **2020**, *193*, 105314. [[CrossRef](#)]

13. Yao, W.; Min, X.; Li, Q.; Wang, Q.; Liu, H.; Liang, Y.; Li, K.; Zhao, Z.; Qu, S.; Dong, Z. Dissociation mechanism of particulate matter containing arsenic and lead in smelting flue gas by pyrite. *J. Clean. Prod.* **2020**, *259*, 120875. [[CrossRef](#)]
14. Tian, F. Experimental research on comprehensive utilization of roasted pyrite. *Multipurp. Util. Miner. Resour.* **2010**, *1*, 38–42.
15. Tugrul, N.; Moroydor Derun, E.; Piskin, M. Utilization of pyrite ash wastes by pelletization process. *Powder Technol.* **2007**, *176*, 72–76. [[CrossRef](#)]
16. Bajwa, D.S.; Pourjashem, G.; Ullah, A.H.; Bajwa, S.G. A concise review of current lignin production applications, products and their environmental impact. *Ind. Crops Prod.* **2019**, *139*, 111536. [[CrossRef](#)]
17. Reed-Hill, R.E.; Abbaschian, R.; Abbaschian, R. *Physical Metallurgy Principles*; Van Nostrand: New York, NY, USA, 1973.
18. Li, H.; Zhu, W.; Yang, J.; Zhang, M.; Zhao, J.; Qu, W. Sulfur abundant S/FeS₂ for efficient removal of mercury from coal-fired power plants. *Fuel* **2018**, *232*, 476–484. [[CrossRef](#)]
19. Li, Y.; Peng, Y.; Wei, Z.; Yang, X.; Gerson, A.D. Crystal face-dependent pyrite oxidation: An electrochemical study. *Appl. Surf. Sci.* **2023**, *619*, 156687. [[CrossRef](#)]
20. Qu, J.; Xie, H.; Song, Q.; Ning, Z.; Zhao, H.; Yin, H. Electrochemical desulfurization of solid copper sulfides in strongly alkaline solutions. *Electrochem. Commun.* **2018**, *92*, 14–18. [[CrossRef](#)]
21. Peters, E. Hydrometallurgical process innovation. *Hydrometallurgy* **1992**, *29*, 431–459. [[CrossRef](#)]
22. Akcil, A.; Ciftci, H. Metals recovery from multimetal sulphide concentrates (CuFeS₂–PbS–ZnS): Combination of thermal process and pressure leaching. *Int. J. Miner. Process.* **2003**, *7*, 233–246. [[CrossRef](#)]
23. Peters, E. Direct leaching of sulfides: Chemistry and applications. *Metall. Mater. Trans. B* **1976**, *7*, 505–517. [[CrossRef](#)]
24. Liu, R.; Jiang, N.W.; Song, Y.F.; Sun, W. Green and efficient comprehensive utilization of pyrite concentrate: A mineral phase reconstruction approach. *Sep. Purif.* **2021**, *276*, 119425. [[CrossRef](#)]
25. Huang, H. A research on acid hot-pressure oxidation pretreatment of a certain refractory gold concentrate. *Gold* **2007**, *28*, 35–39.

Disclaimer/Publisher’s Note: The statements, opinions and data contained in all publications are solely those of the individual author(s) and contributor(s) and not of MDPI and/or the editor(s). MDPI and/or the editor(s) disclaim responsibility for any injury to people or property resulting from any ideas, methods, instructions or products referred to in the content.